HEMATOPOIESIS AND STEM CELLS

Age-dependent effects of *Igf2bp2* on gene regulation, function, and aging of hematopoietic stem cells in mice

Miaomiao Suo,[1] Megan K. Rommelfanger,[2] Yulin Chen,[1] Elias Moris Amro,[1] Bing Han,[1] Zhiyang Chen,[1] Karol Szafranski,[1] Sundaram Reddy Chakkarappan,[3] Bernhard O. Boehm,[4] Adam L. MacLean,[2] and K. Lenhard Rudolph[1,5]

[1]Leibniz Institute on Aging, Fritz Lipmann Institute (FLI), Jena, Germany; [2]Department of Quantitative and Computational Biology, University of Southern California, Los Angeles, CA; [3]Institute of Molecular Medicine, Ulm University, Ulm, Germany; [4]Lee Kong Chian School of Medicine, Nanyang Technological University Singapore, Singapore; and [5]Medical Faculty, Jena University Hospital, Friedrich Schiller University, Jena, Germany

KEY POINTS

- *Igf2bp2* regulates the metabolism- and protein synthesis–related genes necessary for the full function of HSCs in young adult mice.

- Both the activity of *Igf2bp2* at young age and the aging-related loss of *Igf2bp2* gene function contribute to HSC aging.

Increasing evidence links metabolism, protein synthesis, and growth signaling to impairments in the function of hematopoietic stem and progenitor cells (HSPCs) during aging. The *Lin28b/Hmga2* pathway controls tissue development, and the postnatal downregulation of this pathway limits the self-renewal of adult vs fetal hematopoietic stem cells (HSCs). *Igf2bp2* is an RNA binding protein downstream of *Lin28b/Hmga2*, which regulates messenger RNA stability and translation. The role of *Igf2bp2* in HSC aging is unknown. In this study, an analysis of wild-type and *Igf2bp2* knockout mice showed that *Igf2bp2* regulates oxidative metabolism in HSPCs and the expression of metabolism, protein synthesis, and stemness-related genes in HSCs of young mice. Interestingly, *Igf2bp2* expression and function strongly declined in aging HSCs. In young mice, *Igf2bp2* deletion mimicked aging-related changes in HSCs, including changes in *Igf2bp2* target gene expression and impairment of colony formation and repopulation capacity. In aged mice, *Igf2bp2* gene status had no effect on these parameters in HSCs. Unexpectedly, *Igf2bp2*-deficient mice exhibited an amelioration of the aging-associated increase in HSCs and myeloid-skewed differentiation. The results suggest that *Igf2bp2* controls mitochondrial metabolism, protein synthesis, growth, and stemness of young HSCs, which is necessary for full HSC function during young adult age. However, *Igf2bp2* gene function is lost during aging, and it appears to contribute to HSC aging in 2 ways: the aging-related loss of *Igf2bp2* gene function impairs the growth and repopulation capacity of aging HSCs, and the activity of *Igf2bp2* at a young age contributes to aging-associated HSC expansion and myeloid skewing.

Introduction

Metabolic activity contributes to the maintenance of stem cell function by controlling cell proliferation or quiescence, self-renewal, and differentiation.[1-3] However, metabolism, cell growth–controlling pathways, and protein synthesis[4-6] can also lead to functional exhaustion of hematopoietic stem cells (HSCs). Pathways that control metabolism, growth, and protein synthesis may thus have an ambivalent role, in that they control the full functionality of HSCs but at the cost of driving HSC aging. One of the upstream regulators of metabolic activity is the *Lin28/let-7* pathway that controls the expression of cell cycle regulators, mitochondrial protein encoding genes, and glucose metabolism.[7,8] The pathway controls the induction of metabolic pathways and growth signaling, such as IGF, phosphatidylinositol 3-kinase (PI3K), and mTOR.[9] Downstream effectors of the *Lin28/let-7* pathway are *Hmga2* (encoding for a chromatin modifier) and *Igf2bp2* (also known as *Imp2*), which was originally identified as a fetal growth factor and a binding partner of *Igf2* messenger RNA (mRNA).[10,11] Additional targets of IGF2BP2 have been

identified, including major regulators of cellular metabolism and mitochondrial function, such as *Igf1r*, c-*myc*, *Sp1*,[12] *Lamb2*,[13] and *Ucp1*,[14] as well as various noncoding RNAs.[15,16]

In the hematopoietic system, *Lin28* is expressed during development but declines in adult hematopoiesis.[17] The postnatal suppression of *Lin28* limits self-renewal and changes differentiation of HSCs at the transition from fetal to adult hematopoiesis. Overexpression of *Lin28a/b* or its downstream target *Hmga2* enhances the self-renewal capacity of adult HSCs to levels similar to those of fetal HSCs, whereas *Hmga2* knockout abrogates the elevated self-renewal of fetal HSCs.[18,19] In addition, *Lin28* controls fetal B-lymphopoiesis[17] and the differentiation of adult HSCs.[20] However, the possible role of this pathway in HSC aging has not been explored. In this study, we investigated the aging of HSCs in homozygous germline *Igf2bp2*-knockout mice (*Igf2bp2*$^{-/-}$) and wild-type mice (*Igf2bp2*$^{+/+}$). The results reveal a new role of *Igf2bp2* in regulating the expression of metabolism, protein synthesis, and stemness-related genes in HSCs of young mice, which is necessary for young HSCs to have full
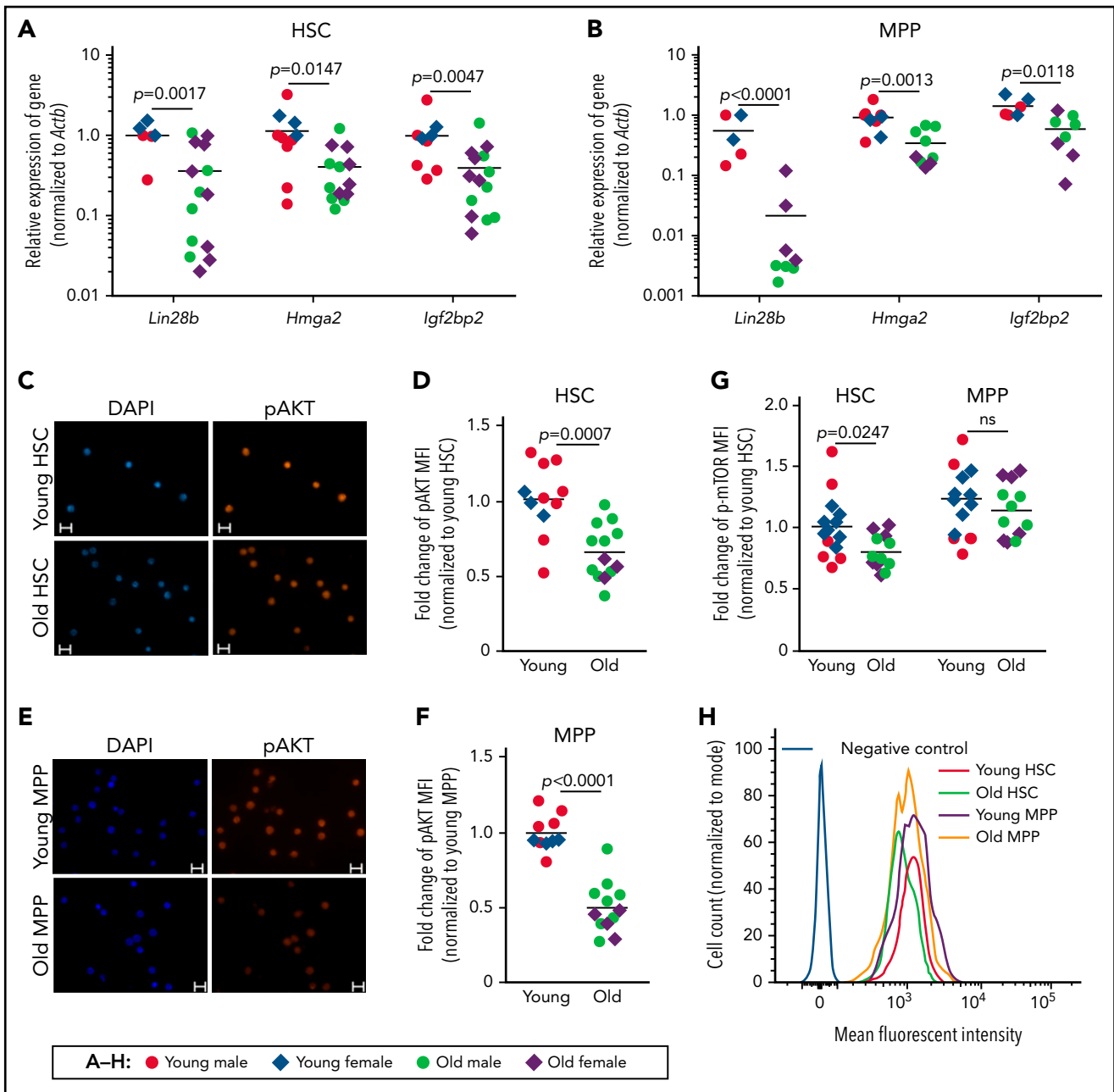
Figure 1. Aged HSCs exhibit decreased expression of *Lin28b-Hmga2-Igf2bp2* mRNAs and reduced activity of the PI3K/AKT/mTOR pathway. Quantitative reverse transcription-polymerase chain reaction (qRT-PCR), immunofluorescence, and fluorescence-activated cell sorting (FACS) analyses of freshly isolated total CD150+ (high and low) HSCs (CD150+CD34−LSK) and MPPs (CD34+LSK) from young mice (range: 3-6 months) and old mice (range: 22-28 months). (A-B) The relative mRNA expression of *Lin28b*, *Hmga2*, and *Igf2bp2* (relative to *Actb*) was analyzed by qRT-PCR in HSCs (A) and MPPs (B). Five to 14 mice per group were analyzed in 2 independent experiments. For each gene and cell type, one sample of young wild-type mice was set to 1 and used as calibrator. Data were log₂ transformed and analyzed by Welch's *t* test. (C-F) Representative micrographs and quantification of the MFI of p-AKT staining in HSCs (C-D) and MPPs (E-F). The MFI of young mice was normalized to 1 for each of the 2 cell populations. A total of 10 to 13 mice per age group were analyzed in 2 independent experiments. Statistical significance was assessed by Welch's *t* test. (C,E) Bars represent 10 μm. (G-H) Quantification and representative FACS profiles of the fluorescence intensity of p-mTOR in HSCs and MPPs. (G) The mean of the MFI of HSCs from young mice was set to 1. A total of 12 to 14 mice per group were analyzed in 2 independent experiments. Statistical significance was assessed by 2-way analysis of variance on log-transformed data followed by pairwise *t* tests with Sidak's correction for multiple comparisons. (H) Representative FACS profiles of HSCs and MPPs from young and old mice. (A-B,D,F-G) Horizontal lines represent the mean of the indicated group. MFI, mean fluorescence intensity; ns, nonsignificant.

colony-forming capacity in culture or to repopulate hematopoiesis in transplant-recipient mice. *Igf2bp2* expression and its gene regulatory function is almost completely lost during aging. The analysis of *Igf2bp2*⁻/⁻ mice indicates that both *Igf2bp2*-dependent gene regulation in young HSCs and the decline of *Igf2bp2*-dependent function in aged HSCs contribute to the development of distinct phenotypes of HSC aging.

Materials and methods

Mice

Igf2bp2-knockout (*Igf2bp2*⁻/⁻) mice carry an inverted exon 3, which leads to a frameshift, a premature stop codon, and a complete knockout of the gene-encoded protein expression (supplemental Figure 1; available on the *Blood* Web site).
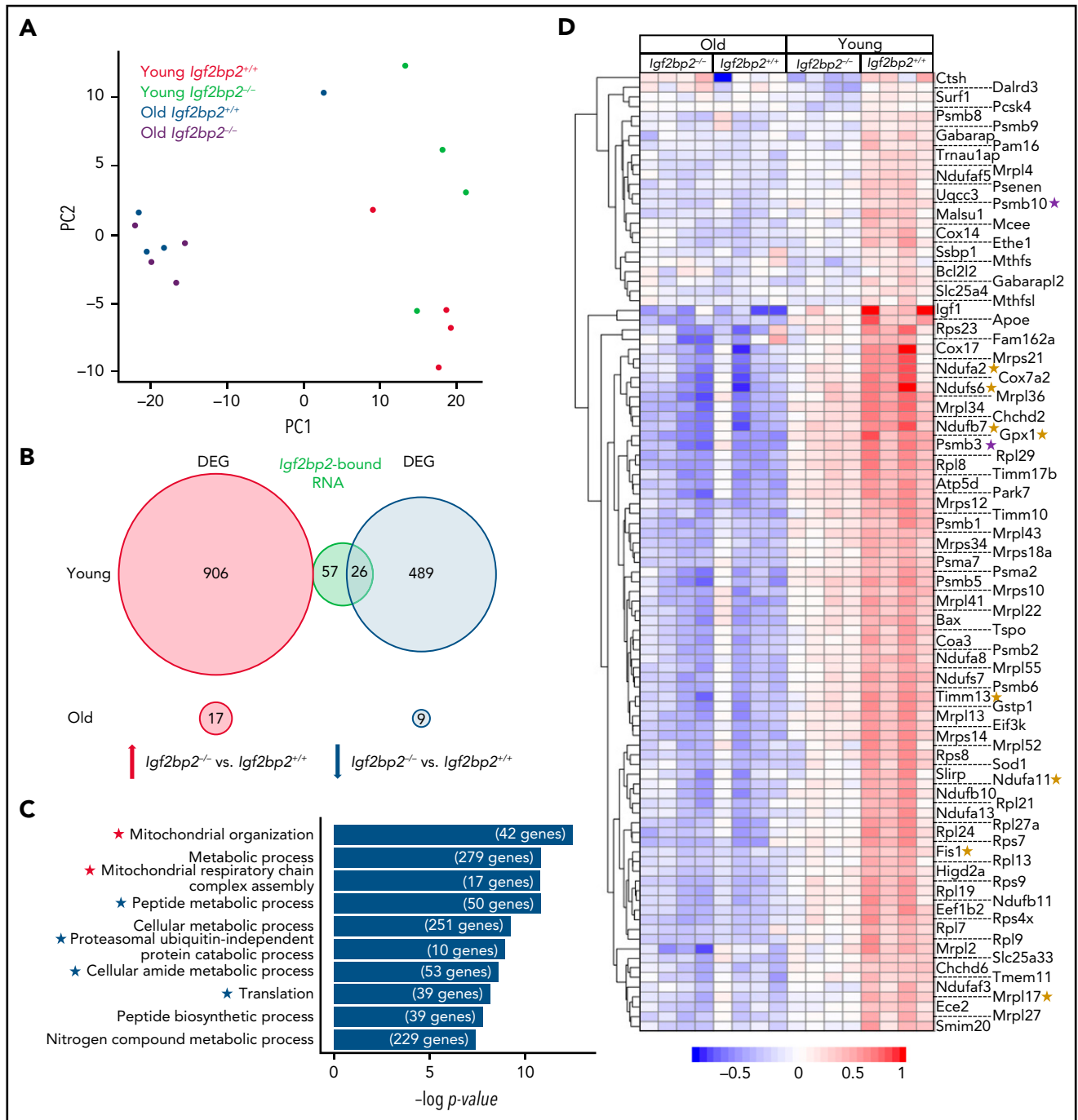
Figure 2. *Igf2bp2* deletion decreases the expression of genes related to mitochondrial metabolism and protein synthesis in young myeloid-biased HSCs. Myeloid-biased HSCs (CD150^high^CD34⁻LSK) were isolated from young (3 months) and aged (range: 22-26 months) *Igf2bp2*^+/+^ and *Igf2bp2*^−/−^ male mice. HSCs from individual mice were analyzed by RNA-seq (n = 4 mice per group). DEGs were identified by the DESeq2 R package (v1.28.1), using the Benjamini-Hochberg–adjusted *P* < .05 as a cutoff. In myeloid-biased HSCs from young *Igf2bp2*^−/−^ vs *Igf2bp2*^+/+^ mice, 1421 DEGs were identified, compared with only 26 DEGs in myeloid-biased HSCs from old *Igf2bp2*^−/−^ vs *Igf2bp2*^+/+^ mice. (A) Principal component analysis (PCA) found that the first PC separated the HSC transcriptomes based on age and that the second PC separated *Igf2bp2* gene status in young mice, but not in the HSCs from old mice. (B) A Venn diagram depicting the number of upregulated (red circle) and downregulated (blue circle) DEGs in myeloid-biased HSCs of *Igf2bp2*^−/−^ vs *Igf2bp2*^+/+^ from young (top) or old (bottom) mice. The DEGs in myeloid-biased HSCs of young *Igf2bp2*^−/−^ vs *Igf2bp2*^+/+^ mice overlapped with 83 mRNAs (green circle) that had been identified to be directly bound by IGF2BP2 in brown fat.[14] Note that mRNA species that are bound by IGF2BP2 exclusively overlapped the downregulated DEGs in myeloid-biased HSCs of *Igf2bp2*^−/−^ vs *Igf2bp2*^+/+^ mice. (C) Bar graph depicts the top 10 GO terms enriched for downregulated DEGs in young *Igf2bp2*^−/−^ mice vs *Igf2bp2*^+/+^ mice (Benjamini-Hochberg correction). The gene number enriched in each term is shown at the end of the bar. Asterisks highlight mitochondria metabolism (red) and protein synthesis-related (blue) GO terms. (D) The heat map shows the expression pattern of all DEGs included in GO terms related to mitochondria metabolism and protein synthesis, as marked by asterisks in panel C. The color scale indicates the expression level. The heat map includes 10 target genes that have been shown to be bound by IGF2BP2 in brown adipose tissue[14] (green circle in panel B) including 8 genes related to mitochondrial metabolism (marked by yellow asterisks) and 2 genes related to protein synthesis (marked by purple asterisks). An analysis of variance was applied to compare the expression of genes shown in the heat map of young *Igf2bp2*^−/−^ myeloid-biased HSCs with old *Igf2bp2*^−/−^ myeloid-biased HSCs (*P* = .26); of young *Igf2bp2*^+/+^ myeloid-biased HSCs with old *Igf2bp2*^+/+^ myeloid-biased HSCs (*P* = .048); or of young *Igf2bp2*^−/−^ myeloid-biased HSCs with old *Igf2bp2*^+/+^ myeloid-biased HSCs (*P* = .49). The *Igf2bp2* deletion makes the expression profile of mitochondria metabolism and protein synthesis–related genes of young myeloid-biased HSCs more similar to that of old myeloid-biased HSCs.
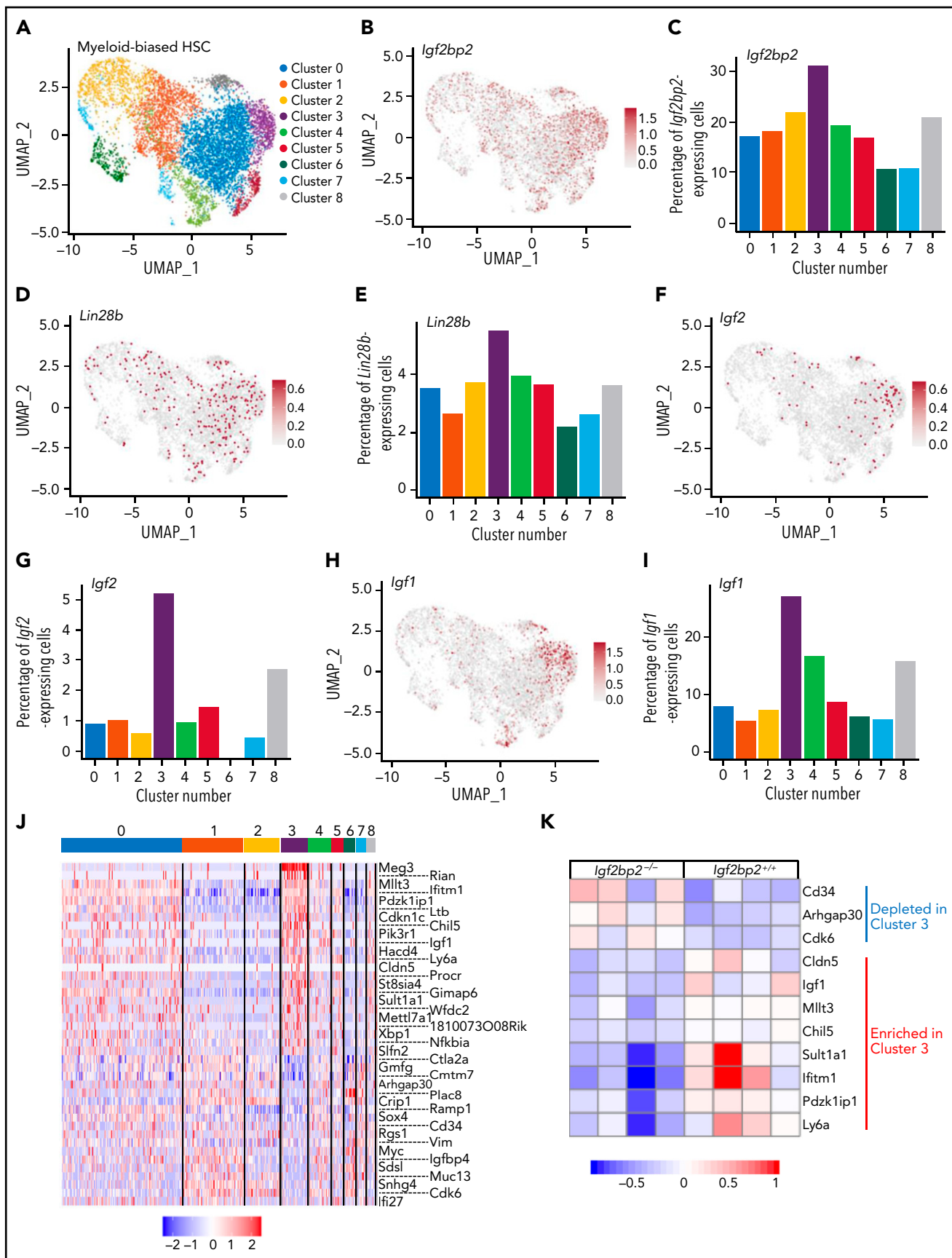
Figure 3.

Flow cytometry

Details of the procedures for cell isolation and staining combination are provided in the supplemental Methods and supplemental Figure 2.

In vivo transplantation assay

Freshly purified HSCs (with marker combinations: 100 HSCs from a young donor or 1000 HSCs from an old donor; CD45.2$^+$) were transplanted into lethally γ-irradiated (12 Gy) recipients (CD45.2$^+$; 4 months old) by IV injection, along with 1×10^6 bone marrow (BM) cells from age-matched competitor mice (CD45.1$^+$). After transplantation, all recipients were treated with antibiotic water (0.01%; enrofloxacin [Baytril]) for 1 week. The chimerism and lineage composition of peripheral blood (PB) and BM of recipient mice was analyzed by fluorescence-activated cell sorting at various time points.

HSC colony-forming assay

Freshly isolated HSCs were seeded in methylcellulose medium (1.2 mL per well in a 6-well plate; M3434; Stem Cell Technologies) at 500 cells per duplicate. For serial rounds of plating, cells harvested from the previous plating were seeded at 5000 cells per duplicate. The number of colonies was scored after 10 days.

Homing assay

A previous protocol[21] was used to examine the homing potential of myeloid-biased HSCs. Details are provided in the supplemental Methods.

Respirometry analysis

Freshly purified HSPCs were used for the Seahorse Cell Mito Stress assay and Real-time ATP Production Assay (Agilent), according to the manufacturer's protocols (supplemental Methods).

Bulk and scRNA-seq

Bulk and single-cell RNA sequencing (scRNA-seq) were performed by the Core Facility Sequencing at Fritz Lipmann Institute (details in supplemental Methods).

Statistical analysis

The numbers of biological replicates and experimental repetitions are stated in the figure legends. Statistical tests and corrections for multiple testing were performed as indicated in the figure legends. The normality of the data, whenever required by the test method, was determined by the Shapiro-Wilk test. The significance level was set at $P \le .05$ for test results, unless otherwise specified. All statistical analyses were performed with GraphPad Prism 7.01 software, except for RNA-seq and proteomic analysis (supplemental Methods) or as specifically indicated.

Lentivirus infection of HSCs, cell culture and inhibitor treatment, MitoRed measurement, and proteomics analysis of *Igf2bp2*-overexpressing stem cells

Details of these experiments and analyses are provided in supplemental Methods.

Results

Lin28b/Hmga2/Igf2bp2 expression and downstream pathways decline in HSPCs during aging

mRNA expression was analyzed in freshly isolated CD150$^+$ (high and low) HSCs (CD150$^+$CD34$^-$LSK) and multipotent progenitors (MPPs; CD34$^+$LSK) of young and old C57Bl/6JRj mice. *Lin28b*, *Hmga2*, and *Igf2bp2* mRNAs were expressed in HSCs and MPPs of young mice, but strongly declined during aging (Figure 1A-B). *Igf2bp2* is a mediator of *Lin28/Hmga2*-regulated metabolic activity and growth.[7] In line with the *Igf2bp2* expression data, immunofluorescence staining of HSPCs revealed a significant reduction in p-AKT in the HSCs and MPPs during aging (Figure 1C-F). In addition, fluorescence-activated cell sorting analysis of p-mTOR expression showed a significant decrease in mTOR activity in aging HSCs but not in MPPs (Figure 1G-H).

Igf2bp2 controls metabolism, protein synthesis, and stemness-related genes in HSCs of young mice, but its function is lost in HSCs of aged mice

In mice, the total population of CD150$^+$ HSCs (CD150$^+$CD34$^-$LSK) can be further separated, based on the level of CD150 expression, into HSCs with myeloid-biased differentiation (CD150^{high}CD34$^-$LSK) or balanced (lymphoid/myeloid) differentiation (CD150^{low}CD34$^-$LSK). Studies have revealed that myeloid-biased (CD150^{high}) HSCs exhibit a more latent repopulation but enhanced self-renewal compared with balanced (CD150^{low}) HSCs.[22] To identify *Igf2bp2*-controlled genes in HSCs, mRNA sequencing was conducted on myeloid-biased HSCs from young and aged *Igf2bp2*$^{-/-}$ vs *Igf2bp2*$^{+/+}$ mice. This subpopulation of HSCs was chosen because it showed the highest expression of *Igf2bp2* (supplemental Figure 3A). In line with results of a previous study,[23] mRNA profiles showed clustering separation of myeloid-biased HSCs from old vs young mice (Figure 2A). Interestingly, *Igf2bp2* gene status separated the clustering of myeloid-biased HSCs from the young mice but not those from the old mice (Figure 2A). Concordantly, a much larger number of differentially expressed genes (DEGs) was identified in myeloid-biased HSCs of *Igf2bp2*$^{-/-}$ vs *Igf2bp2*$^{+/+}$ mice at a young age (1421 DEGs) compared with old age (26 DEGs) (Figure 2B). These data indicate that *Igf2bp2* regulated mRNA expression in

---

Figure 3. *Igf2bp2* expression in young HSCs cosegregates with *Lin28b*, *Igf/Pi3k*, and stemness-related gene expression signatures. Freshly purified myeloid-biased HSCs (CD150^{high}CD34$^-$LSK) from 6-week-old male wild-type mice were analyzed by scRNA-seq (single-pool analysis of n = 5 mice). (A) UMAP plot with Seurat clustering analysis revealing 9 distinct clusters (0-8). (B-I) Feature plots and histograms on target genes of the *Lin28/Igf2bp2* pathway depicting the expression levels and the percentage of positive cells in the HSC subclusters for *Igf2bp2* (B-C), *Lin28b* (D-E), *Igf2* (F-G), and *Igf1* (H-I). Gray dots indicate no expression, and the intensity of the red dots indicates the expression level of each gene. (J) Heat map of DEGs in myeloid-biased HSCs from cluster 3 (enriched for *Igf2bp2* expressing cells) compared with myeloid-biased HSCs from clusters 0, 4, 5, and 8 (Bonferroni-adjusted $P < .01$). The color scale indicates gene expression level. The cluster is enriched for expression of known stemness-related genes (*Mllt3*, *Cdkn1c*, *Procr*, *Xbp1*, and *Slfn2*); for imprinted genes expressed in quiescent-enriched, long-term HSCs[33] (*Meg3*, *Rian*, and *Cdkn1c*); and for positive regulators of *Igf/Akt* signaling (*Pik3r1* and *Igf1*), but is depleted for the expression of inhibitors of *Igf/Akt* signaling (*Cmtm7* and *Igfbp4*). (K) Heat map of the expression pattern of marker DEGs of myeloid-biased HSCs from cluster 3 in panel J that overlapped with the DEGs in young *Igf2bp2*$^{-/-}$ myeloid-biased HSCs vs *Igf2bp2*$^{+/+}$ myeloid-biased HSCs from bulk RNA sequencing analysis (Figure 2). UMAP, Uniform Manifold Approximation and Projection.
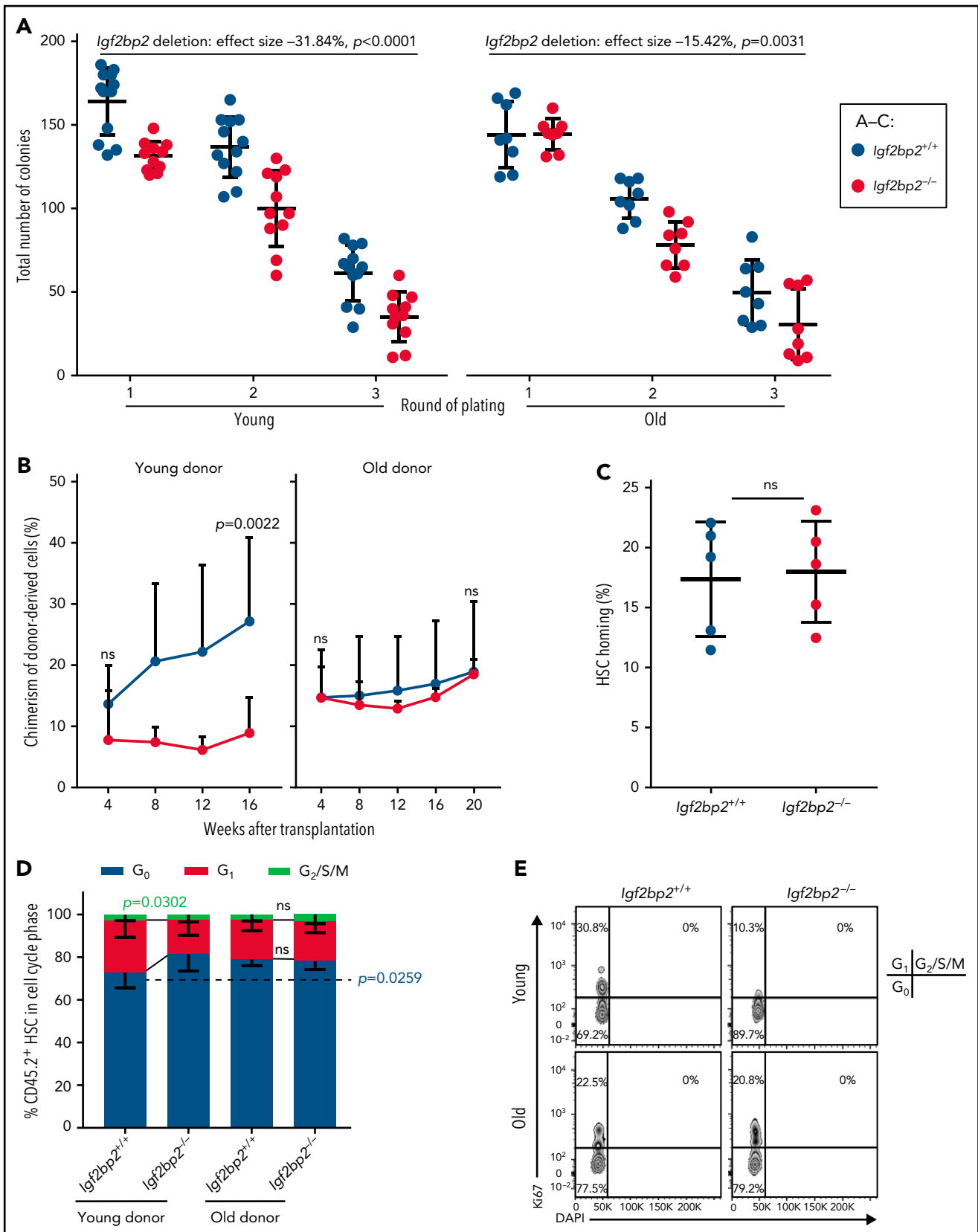

Figure 4. *Igf2bp2* deletion impairs repopulation and colony-forming capacity of young but not old HSCs. Freshly isolated HSCs from *Igf2bp2*^{+/+} and *Igf2bp2*^{−/−} mice were analyzed. (A) Myeloid-biased HSCs (CD150^{high}CD34^{−}LSK; n = 500) from male mice at young age (range: 3-6 months) and old age (range: 22-26 months) were plated for 3 rounds to determine the colony-forming capacity (8-12 mice per group). Statistical analysis by 3-way analysis of variance (ANOVA; using "program package R v3.6.3, function aov()") revealed that age (*P* < .0001), genotype (*P* < .0001), and round of plating (*P* < .0001) significantly affected the colony-forming capacity. Moreover, age and genotype had a significant combinatorial effect (*P* = .0119). Post hoc testing with 2-way ANOVA for separate age groups indicated that

myeloid-biased HSCs of the young mice, but its gene regulatory function was lost during aging.

Because IGF2BP2 is an RNA binding protein that regulates gene expression, we compared the DEGs in myeloid-biased HSCs from $Igf2bp2^{-/-}$ vs $Igf2bp2^{+/+}$ young mice with the mRNAs that were directly bound to IGF2BP2 in mouse brown fat.[14] We found that they exclusively overlapped with downregulated but not with upregulated DEGs in myeloid-biased HSCs of young $Igf2bp2^{-/-}$ vs $Igf2bp2^{+/+}$ mice (Figure 2B), suggesting that upregulated genes in response to $Igf2bp2$ deletion may represent secondary responses and not direct IGF2BP2 targets. Further analysis focused on mRNA that showed decreased expression in $Igf2bp2^{-/-}$ vs $Igf2bp2^{+/+}$ myeloid-biased HSCs. Gene Ontology (GO) analysis revealed a significant reduction in the expression of genes related to the GO terms "mitochondrial metabolism" and "protein synthesis" in $Igf2bp2^{-/-}$ vs $Igf2bp2^{+/+}$ myeloid-biased HSCs of young mice, but not in those of old mice (Figure 2C-D). Analysis of variance (ANOVA) of this DEG subset showed that the expression of these genes significantly declined in myeloid-biased HSCs from aged vs young $Igf2bp2^{+/+}$ mice (Figure 2D; $P = .048$). However, there was no significant difference in the expression of these genes in myeloid-biased HSCs from aged $Igf2bp2^{+/+}$ vs $Igf2bp2^{-/-}$ mice ($P = .49$). These data indicate that $Igf2bp2$ controls the expression of genes related to metabolism and protein synthesis in myeloid-biased HSCs of young mice, but this gene regulatory function of $Igf2bp2$ is lost during aging.

$Igf2bp2$ expression is enriched in a subcluster of HSCs from young mice cosegregating with expression of $Lin28$, $Igf/Pi3k$, and stemness-related genes

scRNA-seq was conducted on freshly isolated myeloid-biased HSCs from a pool of 6-week-old, male, wild-type mice (n = 5). Mice of this age and sex were chosen, because they showed the highest expression of $Igf2bp2$ (supplemental Figure 3B-C). Through cell clustering (via the Louvain algorithm in Seurat), scRNA-seq identified a subcluster (cluster 3) of myeloid-biased HSCs that had an increased percentage of $Igf2bp2$-expressing cells compared with the other 8 subclusters that were identified by specific markers of each cluster (Figure 3A-C; supplemental Figure 4A). In agreement with this observation, cluster 3 was also enriched for an increased percentage of cells expressing other components of the Lin28 pathway (Figure 3D-E; supplemental Figure 4B-C), as well as downstream targets that are known to be bound and regulated by $Igf2bp2$ (Figure 3F-I).

Next, the gene expression in cluster 3 was compared with that in 4 other clusters (0, 4, 5, and 8; Figure 3A). These clusters were selected based on their similarity to cluster 3 as unbiased and unprimed toward particular hematopoietic lineages. The 4 remaining clusters (1, 2, 6, and 7) were excluded from the

comparison, as they expressed genes that indicate priming toward lineage commitment (megakaryocyte/thrombocyte and erythroid lineages; supplemental Figure 5A-H). $Igf2bp2$ expression in cluster 3 was significantly upregulated ($P = 4.142 \times 10^{-9}$; supplemental Figure 5I) when compared with individual, unprimed clusters 0 ($P = 2.6 \times 10^{-9}$), 4 ($P = 6.6 \times 10^{-4}$), and 5 ($P = 8.7 \times 10^{-4}$). Only when compared with cluster 8 was the difference not significant ($P = .07$), but interestingly, cluster 8 had an expression profile of genes that was more similar to that of cluster 3 than to that of the other clusters (Figure 3J). Compared with the unprimed HSC clusters (0, 4, 5, and 8), the expression signature of cluster 3 showed an upregulation of IGF/PI3K signaling ($Igf1$, $Pik3r1$) and a downregulation of inhibitors of AKT signaling ($Igfbp4$ and $Cmtm7$; Figure 3J). IGF/PI3K/AKT represent major regulators of cellular metabolism and growth that are known to be activated by $Igf2bp2$-mediated RNA expression.[24-27] Interestingly, cluster 3 was also enriched for the expression of genes related to quiescence and stemness of HSCs, including $Mllt3$,[28] $Cdkn1c/p57$,[29] $Procr$,[30] $Xbp1$,[31] and $Slfn2$[32] (Figure 3J). Moreover, cluster 3 showed enrichment for genes that are known to be regulated by imprinting and highly expressed in quiescent-enriched, long-term HSCs,[33] including $Rian$, $Cdkn1c/p57$, $H19$, and $Meg3$[34] (Figure 3J; supplemental Figure 4D-I). The connection between $Igf2bp2$ expression in cluster 3 with the marker genes in this cluster was supported by a comparison of the cluster 3 marker genes with the pooled RNA-seq data on myeloid-biased HSCs of young $Igf2bp2^{-/-}$ vs $Igf2bp2^{+/+}$ mice (Figure 2). This analysis revealed that the marker genes of cluster 3 that overlapped with DEGs in the RNA-seq analysis of pooled myeloid-biased HSCs from $Igf2bp2^{-/-}$ vs $Igf2bp2^{+/+}$ mice were all regulated in the expected direction (Figure 3K).

$Igf2bp2$ deletion impairs the functional capacity of HSCs from young mice more than HSCs from aged mice

The colony-forming capacity of HSCs was determined by using freshly isolated myeloid-biased HSCs and balanced HSCs from $Igf2bp2^{-/-}$ and $Igf2bp2^{+/+}$ young and old male mice. $Igf2bp2$ deletion inhibited the colony-forming capacity of myeloid-biased HSCs, and the effect size of $Igf2bp2$ deletion on inhibition of colony-forming capacity was higher for myeloid-biased HSCs from young than for aged mice (Figure 4A). Similar results were obtained for balanced HSCs, albeit the effect size of the $Igf2bp2$ genotype was reduced overall (supplemental Figure 6).

The in vivo repopulation capacity of HSCs was assessed by transplantation of freshly isolated myeloid-biased HSCs from young mice. For old mice, CD150$^+$ (high and low) HSCs were used. $Igf2bp2$ deletion significantly reduced the repopulation capacity of young myeloid-biased HSCs during long-term engraftment in primary recipients (Figure 4B; left). In contrast, $Igf2bp2$ gene status did not affect the long-term repopulating

Figure 4 (continued) $Igf2bp2$ deletion had a stronger effect on impairing the colony-forming capacity of myeloid-biased HSCs from young mice (effect size: −31.84 units; $P < .0001$) compared with aged mice (effect size: −15.42 units; $P = .0031$). (B,D-E) Myeloid-biased HSCs (CD150^{high}CD34$^-$LSK; n = 100) from young donors (3-6 months) or 1000 total CD150$^+$ (high and low) HSCs (CD150$^+$CD34$^-$LSK) from old donors (27 months) were transplanted along with 1 × 10^6 competitor BM cells (CD45.1). Young HSCs, 9-10 donors and recipients (1:1 transplantation) per group; old HSCs, 4 to 5 recipient per group. (B) Analysis of the total chimerism of donor-derived cells in PB at the indicated time points after transplantation. (D-E) Donors were analyzed 16 or 20 weeks after transplantation. Cell cycle status of donor-derived HSCs: quantification (D) and representative fluorescence-activated cell sorting plots (E). (C) Percentage of homed myeloid-biased HSCs (CD150^{high}CD34$^-$LSK) from 3-month-old $Igf2bp2^{-/-}$ vs $Igf2bp2^{+/+}$ donor mice (n = 5 mice per group). (B-D) Statistical significance of genotype-dependent difference in young or old donors was determined by Welch's t test. All data are expressed as the mean ± SD; ns, nonsignificant.
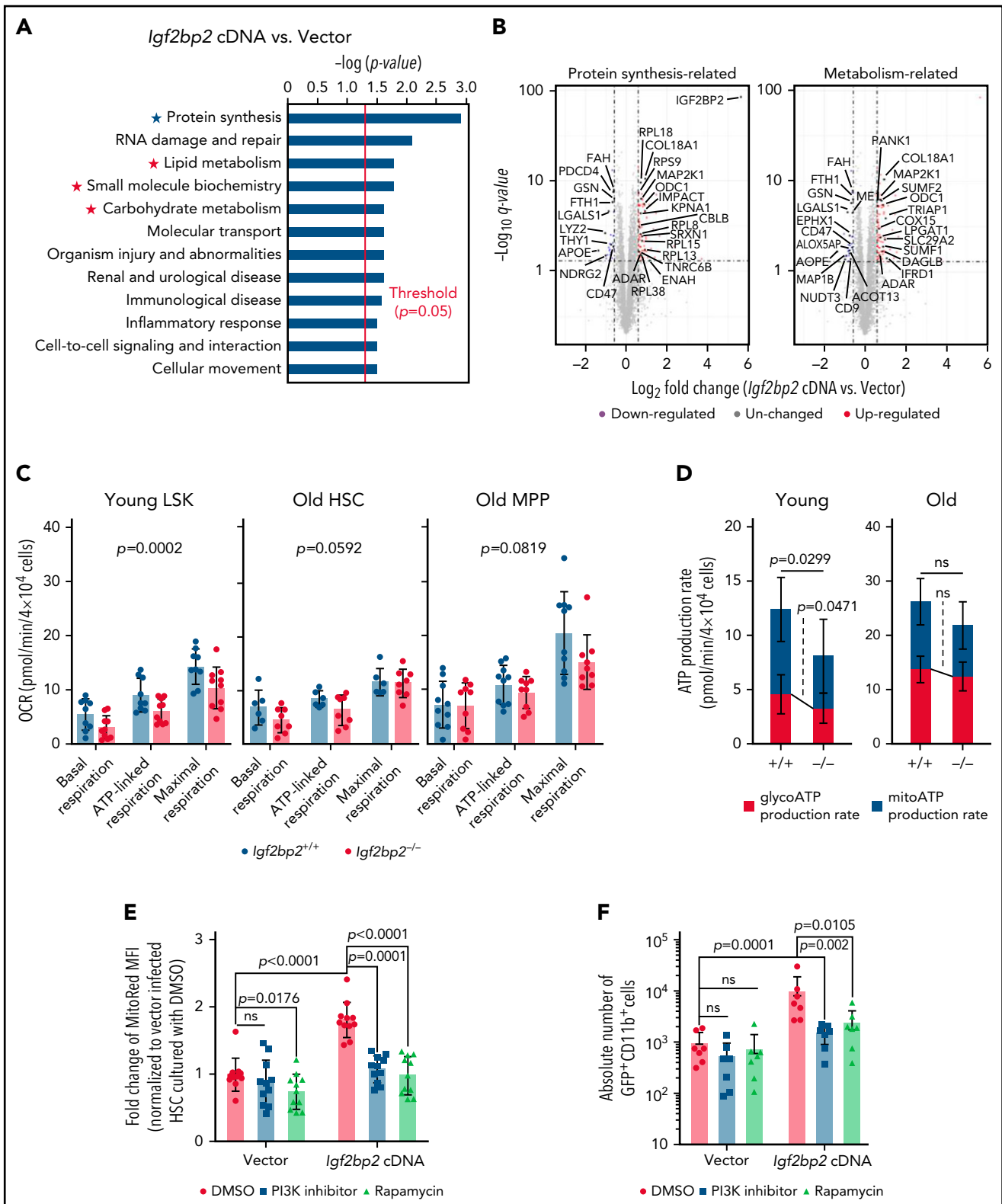
Figure 5. *Igf2bp2* regulates mitochondrial activity in HSPCs of mice. (A-B) Freshly isolated, total CD150+ (high and low) HSCs (CD150+CD34–LSK) from wild-type males (range: 24-27 months) were virally infected with *Igf2bp2* cDNA or an empty vector (control). After transduction (2.5 days), transduced cells (CD48–LSKs) were re-sorted for proteomics analysis (n = 5 replicates per group). (A) Ingenuity Pathway Analysis (IPA) on differentially expressed proteins, Fisher's exact test with Benjamini-Hochberg–corrected P values. (B) The differentially expressed proteins related to protein synthesis (marked by blue asterisks) metabolism (marked by red asterisks). Volcano plots on differentially expressed proteins related to protein synthesis (left, marked by blue asterisks in panel A) and metabolism (right, marked by red asterisks in panel A) in *Igf2bp2*-overexpressing cells compared with control cells. Relative quantification was performed in Spectronaut for each pairwise comparison using the replicate samples from each condition. (C-D) Freshly isolated LSK (lineage–cKit+Sca1+) from young mice (range: 3-6 months) and total CD150+ (high and low) HSCs (CD150+CD34–LSK) and multipotent progenitors (CD34+LSKs = MPPs) from old mice (range: 22-26 months) were used for respirometry analysis of *Igf2bp2*–/– vs *Igf2bp2*+/+ mice. (C) Quantification of oxygen

capacity of CD150+ HSCs of aged mice (Figure 4B; right). Based on the difference in purification of test donor HSCs, we cannot exclude that the transplantation of purified myeloid-biased (CD150high) HSCs could have revealed an inhibitory effect of *Igf2bp2* deletion on the repopulation function of myeloid-biased HSCs from old mice. However, the analysis of colony-forming capacity demonstrated that *Igf2bp2* deletion had a stronger inhibitory effect on the function of myeloid-biased HSCs from young mice vs those from old mice. *Igf2bp2* gene status had no effect on the homing capacity of myeloid-biased HSCs (Figure 4C), as measured by previously established protocols.[21] However, *Igf2bp2* deletion led to an increase in the fraction of young donor–derived HSCs (CD150+) in quiescence (G_0) and a decrease in those in G_1 (Figure 4D-E). In aged donor HSCs (CD150+), *Igf2bp2* gene status had no effect on those cell cycle parameters (Figure 4D-E). Together, these data indicate that *Igf2bp2* is necessary for full repopulation function and colony-forming capacity of young, myeloid-biased HSCs, but the deletion of *Igf2bp2* has lesser effects on the function of aged HSCs.

Igf2bp2 regulates mitochondrial metabolism and protein synthesis of HSCs

The experiments described so far showed that *Igf2bp2* activated the expression of genes necessary for mitochondria metabolism and protein synthesis in HSCs (Figure 2). To further validate this result, we conducted a proteomics analysis on *Igf2bp2*-overexpressing vs control HSCs (supplemental Figure 7A-B) on HSCs of aged mice, given that we had observed a reduction in *Igf2bp2* gene expression and a loss of its gene regulatory function during HSC aging (Figures 1 and 2). Ingenuity Pathway Analysis of differentially expressed proteins identified EIF2 activation as the single, significantly enriched pathway in *Igf2bp2* cDNA-expressing HSCs vs controls ($P = .026$). EIF2 controls a rate-limiting step in translation initiation.[35] Downregulation of protein synthesis is essential for maintenance of BM HSCs.[6,36] Ingenuity Pathway Analysis of enriched terms related to biological functions in the set of differentially expressed proteins confirmed a strong induction of the term protein synthesis in *Igf2bp2*-overexpressing HSCs vs controls and, in addition, an enrichment of metabolism-related terms (Figure 5A-B).

To determine the functional impact of the endogenous expression level of *Igf2bp2* on mitochondria metabolism, respirometry analysis was conducted on freshly isolated HSPCs from young and aged *Igf2bp2*−/− and *Igf2bp2*+/+ mice. Because of the number of cells needed, this experiment was conducted on LSK cells from young mice (containing a mean of 90% MPPs and 7% HSCs in this experiment) and on CD150+ (high and low) HSCs and MPPs from old mice. *Igf2bp2* depletion had a stronger effect on lowering the mitochondrial respiration (basal, ATP-linked, and maximal) of young LSK cells (3.117 ± 1.081 units; $P = .0002$

compared with that of aged HSCs (1.548 ± 1.113 units; $P = .0592$) or MPPs (2.339 ± 1.835 units; $P = .0819$; Figure 5C; supplemental Figure 7). *Igf2bp2* deletion also led to a reduction of adenosine triphosphate (ATP) production in LSK cells of mice, which was not seen at a significant level in aged HSCs (Figure 5D). *Igf2bp2*-dependent lowering of the oxygen consumption rate of young LSK cells did not lead to changes in ROS levels (supplemental Figure 7D). However, GO terms that were significantly enriched and downregulated overall in the bulk RNA sequencing of myeloid-biased HSCs of young *Igf2bp2*−/− vs *Igf2bp2*+/+ mice (Figure 2) included 20 GO terms in the list of the top 200 significant GO terms that were related to mitochondrial stress (supplemental Figure 7E; supplemental Table 1; for GO-terms that were significantly enriched and upregulated overall in the same experiment, see supplemental Table 2). Together, it appears that mitochondrial stress was enhanced in young *Igf2bp2*+/+ vs *Igf2bp2*−/− myeloid-biased HSCs, despite the lack of detectable, genotype-related differences in ROS, possibly because of the lack of sensitivity of the currently used dye-based methodology. Interestingly, intracellular ATP concentration also did not show a reduction in CD150+ (high and low) HSCs and in MPPs of young *Igf2bp2*−/− mice vs wild-type mice (supplemental Figure 7F), despite the observed genotype-dependent differences in ATP production rates (Figure 5D). It is possible that the inhibitory effect of *Igf2bp2* deletion on protein synthesis (Figure 2) reduces ATP consumption, thus outweighing reduction in ATP synthesis in *Igf2bp2* depleted cells.

The *Lin28/let-7* pathway is upstream of *Hmga2/Igf2bp2* in regulating cell growth, protein synthesis, and metabolism by activation of mTOR and PI3K pathways.[9] To test whether this pathway contributes to *Igf2bp2*-mediated differentiation of HSCs in culture, *Igf2bp2*-cDNA vs control vector–infected CD150+ (high and low) HSCs were treated with inhibitors of mTOR (by rapamycin) or PI3K signaling (by LY294002). In culture, freshly isolated HSCs differentiate mainly into the myeloid lineage (CD11b+), thus reflecting the HSC's capacity for such differentiation. Both inhibitors abrogated *Igf2bp2*-overexpression–induced increases in the mitochondrial membrane potential (Figure 5E) and in the induction myeloid differentiation of HSCs (Figure 5F). Together, these results showed that iatrogenic induction of *Igf2bp2* activates mitochondria, protein synthesis pathways, and differentiation of HSCs in an mTOR/PI3K-dependent manner.

Enhanced mitochondrial and mTOR activity can lead to loss of HSC maintenance.[37,38] To determine consequences of *Igf2bp2* overexpression, freshly isolated CD150+ (high and low) HSCs from young and aged mice were transplanted, along with competitor cells, into lethally irradiated recipients. Twelve weeks after transplantation, PB analysis revealed a significant loss of repopulation capacity (supplemental Figure 8A-B) and

Figure 5 (continued) consumption rates (OCRs) for basal respiration, ATP-linked respiration and maximal respiration of cells of the indicated genotype and age (young LSK cells, 9-10 mice per genotype, 2 independent experiments; old HSCs, 6 to 8 mice per genotype, 2 independent experiments; and old MPPs, 9 to 10 mice per genotype, 3 independent experiments). Linear modeling and analysis of variance (ANOVA; using "program package R v3.6.3, function aov()") on genotype and all respirometric parameters revealed a significant reduction of the OCR in LSK cells of young mice ($P = .0002$) but not in HSCs ($P = .0592$) or MPPs ($P = .0819$) of old mice. (D) Histogram of the ATP production rate. Young LSKs (left): 11 to 13 mice per genotype, 4 independent experiments; old HSCs (right), 8 to 11 mice per genotype, 3 independent experiments. Statistical analysis was performed with Welch's *t* test. (E-F) Transduced HSCs were cultured with dimethyl sulfoxide (DMSO; control; circles) or inhibitors of PI3K (squares) or rapamycin (triangles) starting 12 hours after transduction. (E) The mitochondrial potential of transduced CD48− LSK cells was determined 2 days after culture initiation by MitoRed fluorescence-activated cell sorting (FACS) analysis. The mean fluorescence intensity of MitoRed was normalized to DMSO treated, vector-transduced cells set to 1. A total of 11 mice per group in 3 independent experiments. (F) The absolute number of DAPI−GFP+CD11b+ cells in the indicated groups was analyzed 7 days after culture initiation by FACS (n = 7 mice per group in 3 independent experiments). (E-F) Statistical analysis by 2-way ANOVA on log-transformed data followed by pairwise *t* tests with Sidak's correction for multiple comparisons. All data are expressed as the mean ± SD; ns, nonsignificant.
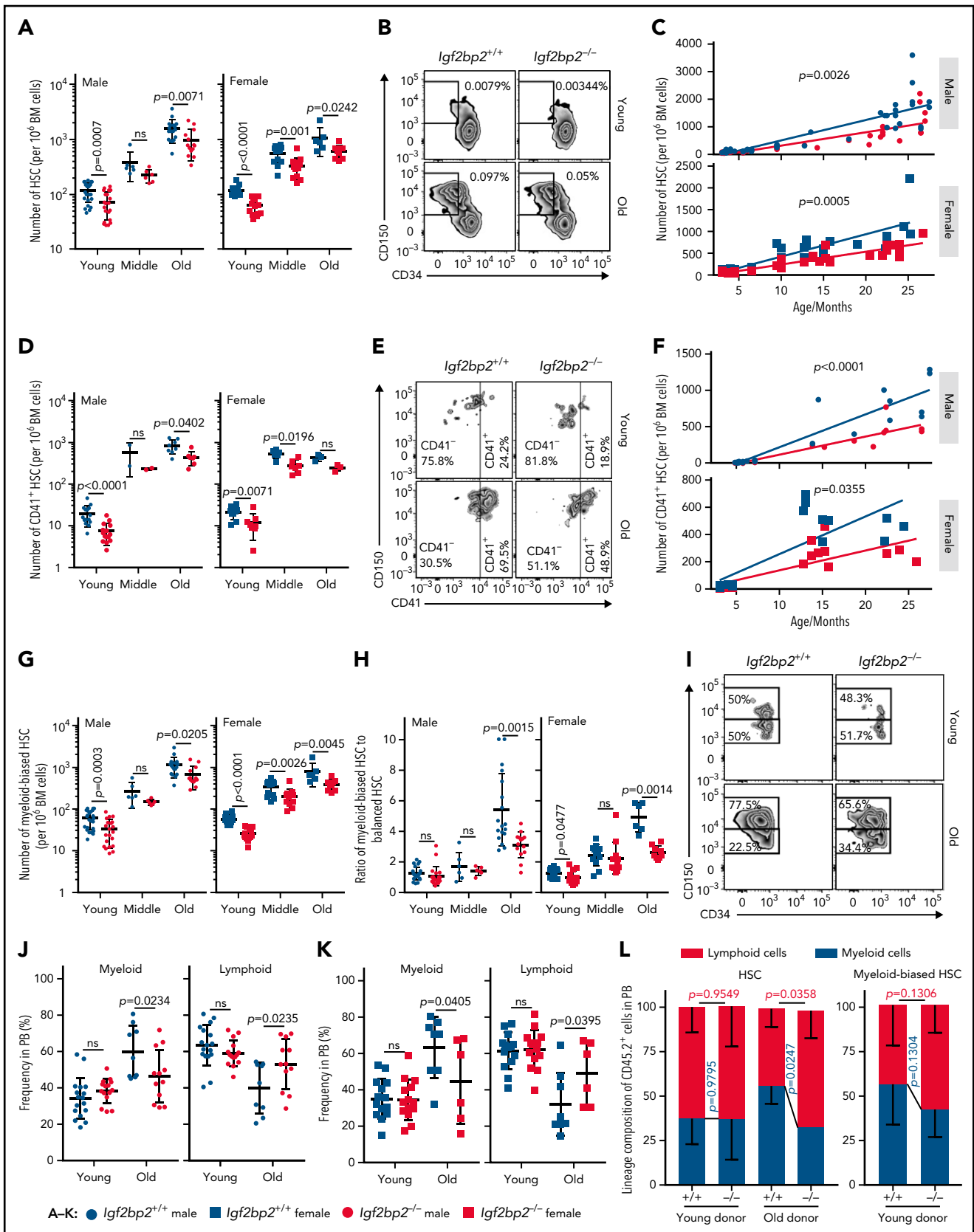
Figure 6. *Igf2bp2* deletion ameliorates aging-associated myeloid-biased HSC expansion and myeloid skewing in PB. Fluorescence-activated cell sorting (FACS) analysis of the frequencies of CD150+ (high and low) HSCs (CD150+CD34− LSK) (A-C), myeloid-restricted HSCs (CD41+CD150+CD34− LSK) (D-F), and myeloid-biased (CD150high CD34− LSK) (G-H) vs balanced HSCs (CD150low CD34− LSK) in total BM cells from *Igf2bp2*+/+ and *Igf2bp2*−/− mice at young (range: 3-6 months), middle (range: 9-15 months), and old (range: 18-27 months) age. (A,D,G) Graphs show the number of HSCs per 10⁶ total BM cells. Data points represent 6 to 24 individual

aggravated myeloid skewing (supplemental Figure 8C) in recipients of HSCs overexpressing *Igf2bp2* compared with controls, especially when HSCs from aged mice were transplanted. These results indicate that overexpression of *Igf2bp2* cannot rescue the function of HSC from aged mice but leads to HSC exhaustion, possibly related to the supraphysiological induction of mitochondria and PI3K/mTOR activity.

Igf2bp2 deletion ameliorates aging-associated HSC expansion and myeloid skewing

Increases in the number of phenotypic HSCs represent a hallmark of the aging hematopoietic system in mice and humans.[39-42] In this study, the number of phenotypic-defined HSCs was investigated in young (range: 3-6 months), middle (range: 9-15 months), and old (range: 18-27 months) *Igf2bp2*^{+/+} and *Igf2bp2*^{−/−} mice. In agreement with previous results,[14] there was a reduction in body weight and an elongated lifespan in *Igf2bp2*^{−/−} mice vs *Igf2bp2*^{+/+} littermate controls (supplemental Figure 9).

Analysis of the number of CD150^{+} (high and low) HSCs revealed the expected increase in the number of HSCs during aging (Figure 6A-B). *Igf2bp2* deletion significantly reduced this age-related increase in HSCs in male and female mice (Figure 6A-B). In addition, the slope of the increase in HSC numbers from young adult to old age was also significantly lower in *Igf2bp2*^{−/−} vs *Igf2bp2*^{+/+} mice (Figure 6C), implying that *Igf2bp2* gene status affects aging-related increases in the number of HSCs. Moreover, *Igf2bp2* deletion ameliorated aging-associated increases in CD41^{+} HSCs (Figure 6D-F), a subpopulation of myeloid-primed HSCs exhibiting megakaryocyte-erythroid–directed differentiation and strong aging-associated increases.[43-45] Similarly, *Igf2bp2* deletion reduced the aging-related increase in the number of myeloid-biased (CD150^{high}) HSCs[46] in mice of both sexes (Figure 6G). *Igf2bp2* gene status did not affect the aging-related increase in balanced HSCs (CD150^{low}) and reduced the age-dependent increase in the number of CD41^{−} HSCs only in male mice (supplemental Figure 10A-B). *Igf2bp2* deletion also led to a significant reduction in the ratio of myeloid-biased HSCs vs balanced HSCs in aged *Igf2bp2*^{−/−} vs *Igf2bp2*^{+/+} mice of both sexes (Figure 6H-I). *Igf2bp2* gene status had no effect on progenitor cell populations, such as MPPs, MPP subpopulations, common myeloid progenitors (CMP), and total BM cells (supplemental Figure 10C-F). Only the number of common lymphoid progenitors (CLP) was reduced in young (both sexes) and middle-aged (male) *Igf2bp2*^{−/−} vs *Igf2bp2*^{+/+} mice (supplemental Figure 10G). *Igf2bp2*^{−/−} vs *Igf2bp2*^{+/+} mice did not show a reduction in MPP4 cells (supplemental Figure 10D). Because

MPP4s represent a subpopulation of MPPs primed to undergo lymphoid differentiation,[47,48] it is conceivable that *Igf2bp2* is necessary for MPP4s to generate CLP.

To analyze consequences of *Igf2bp2* deletion on myeloid skewing, PB samples from young and aged *Igf2bp2*^{−/−} vs *Igf2bp2*^{+/+} mice were analyzed. *Igf2bp2* deletion partially rescued aging-associated myeloid skewing in blood cell production resulting in an improved balance of myeloid-to-lymphoid cells in the PB of aged mice of both sexes (Figure 6J-K). To determine whether HSC-intrinsic mechanisms contribute to this rescue, an HSC transplantation experiment was conducted using CD150^{+} (high and low) HSCs. As expected from previous studies,[43,45] the ratio of myeloid to lymphoid cells was elevated after transplantation of CD150^{+} (high and low) HSCs from aged vs young donor mice (Figure 6L; left graph). Although it did not affect the ratio of myeloid to lymphoid cells in recipients of HSCs from young donors, *Igf2bp2* deletion rescued myeloid skewing in donor-derived PB cells of recipients of HSCs from old donors (Figure 6L; left; supplemental Figure 10H). When purified, myeloid-biased (CD150^{high}) HSCs from young donors were used for transplantation (Figure 6L; right), the myeloid skewing in transplant recipients was similar to that in recipients of CD150^{+} HSCs from aged mice (Figure 6L; left), and it was not significantly altered by *Igf2bp2* deletion (Figure 6L; right graph). Together, these results indicate that the ameliorated increase in the ratio of myeloid-biased to balanced HSCs in aged *Igf2bp2*^{−/−} vs *Igf2bp2*^{+/+} mice (Figure 6H) contributes to the reduction in myeloid skewing in the PB of *Igf2bp2*^{−/−} vs *Igf2bp2*^{+/+} mice.

Discussion

This study reveals experimental evidence that in young HSCs, the endogenous physiological expression level of *Igf2bp2* regulates mitochondrial metabolism and the expression of genes related to metabolism and protein synthesis. *Igf2bp2* is necessary for the full function of young myeloid-biased HSCs to form colonies in culture and to repopulate recipients in transplantation experiments. The effect of *Igf2bp2* gene status on these functional parameters of HSCs is strongly reduced during aging, which coincides with age-related downregulation of *Igf2bp2* expression. Importantly, germline knockout of *Igf2bp2* leads to aging-like phenotypes of HSCs in young mice, including the loss of *Igf2bp2*-dependent gene regulation and impairments in colony forming and in vivo repopulation capacity of HSCs. Mechanistically, the loss of *Igf2bp2*-dependent regulation of metabolism-, cell growth–, and protein synthesis–related genes appears to contribute to the functional decline of *Igf2bp2*^{−/−} vs

Figure 6 (continued) mice per group. (B,E,I) Representative FACS plots. (C,F) Scatter plots depict the number of HSCs per 10^6 total BM cells. The slopes were analyzed by linear regression; group-wise (dis)agreement of models was determined with a Wald test (C), regression coefficients $R^2 = 0.7517$ for *Igf2bp2*^{+/+} male mice, $R^2 = 0.7174$ for *Igf2bp2*^{−/−} male mice; $R^2 = 0.709$ for *Igf2bp2*^{+/+} female mice, and $R^2 = 0.8576$ for *Igf2bp2*^{−/−} female mice; (F) $R^2 = 0.851$ for *Igf2bp2*^{+/+} male mice, $R^2 = 0.8504$ for *Igf2bp2*^{−/−} male mice $R^2 = 0.6363$ for *Igf2bp2*^{+/+} female mice, and $R^2 = 0.5988$ for *Igf2bp2*^{−/−} female mice. (H) Ratio of myeloid-biased HSCs to balanced HSCs of mice of the indicated age group, sex, and genotype. (J-K) The frequency of myeloid cells (including Gr1^{+} cells and CD11b^{+} cells) and lymphoid cells (including B220^{+}, CD4^{+}, and CD8^{+} cells) in PB of the indicated genotypes of male (J) and female (K) mice at young (range: 3-6 months) and old (range: 22-27 months) ages. Data points represent 6 to 17 mice per genotype per age. (A,D,G-H,J-K) Statistics were calculated by 2-way analysis of variance on log-transformed data (A,D,G), on logit-transformed data (H), or on original data (J-K), followed by Sidak's test for multiple comparisons. The y-axes of panels A, D, and G are in log scale. (L) HSCs from young (range: 3-6 months) or old (27 months) donors were transplanted along with competitor total BM cells (CD45.1). Analysis of myeloid cells (including Gr1^{+} and CD11b^{+} cells) vs lymphoid cells (including B220^{+}, CD4^{+}, and CD8^{+} cells) in donor-derived cells in PB 16 or 20 weeks after transplantation. Lineage composition in donor-derived PB of recipients of CD150^{+} (high and low) HSCs from young and old donors (4-5 mice per group; left). Lineage composition in donor-derived PB of recipients of myeloid-biased HSCs (right; CD150^{high}) from young donors (9-10 mice per group; right). Note the myeloid skewing in transplantation of CD150^{+} (high and low) HSCs from old donors was rescued by *Igf2bp2* depletion. Statistical significance of genotype-dependent differences between young and old donors was calculated by Welch's *t* test. Data are expressed as the mean ± SD. ns, nonsignificant.

$Igf2bp2^{+/+}$ HSCs at young age, as well as to the reduction in HSC function in aged mice. In line with this interpretation, the study revealed significant effects of the endogenous $Igf2bp2$ gene status on mitochondrial respiration of freshly isolated HSPCs of young mice but not of old mice. Together, the age-dependent loss of gene regulatory function of $Igf2bp2$ may contribute to the aging-related impairments of HSC function related to declines in metabolism and protein synthesis. In contrast to our study, $Igf2bp2$ has been reported to suppress the expression of mitochondrial protein–encoding mRNA in HSCs of young mice via stabilization of the m6A RNA of Bmi1.[49] However, our reanalysis of the publicly available RNA sequencing data of that study[49] did not verify the conclusion that $Igf2bp2$ suppresses mitochondria protein–encoding genes (supplemental Figure 11).

Unexpectedly, despite the loss of $Igf2bp2$ gene function in aging, this study shows that $Igf2bp2$-deletion ameliorates 2 of the other hallmark phenotypes of HSC aging: the aging-associated increase in myeloid-biased HSCs and the bias of aged HSCs to regenerate myeloid blood cells in aged mice and in recipient mice of transplanted HSC from aged mice of both genotypes. We cannot exclude the possibility that the deletion of the remaining activity of $Igf2bp2$ in HSC of aged knockout mice could have an effect on these HSC aging phenotypes. However, the strong reduction of the gene regulatory function of $Igf2bp2$ in HSCs of aged mice supports the conclusion that $Igf2bp2$ activity in young HSCs contributes to the development of HSC aging phenotypes at old age. In the current study, we used a germline $Igf2bp2$ knockout model; the observed effect of $Igf2bp2$ gene status on HSC aging may even involve effects of $Igf2bp2$ on fetal HSCs. The results of the current study indicate that residual activity of the developmental $Lin28/Hmga2/Igf2bp2$ pathway contributes to HSC function at young adult age, but the activity of this pathway is lost during aging, and this decline by itself represents an integral component of HSC aging. Moreover, the findings support the concept that the activity of developmental pathways during early life influences the development of aging phenotypes in late life.

Acknowledgment

Authorship

Contribution: M.S. designed and performed the majority of experiments and analyses with help from E.M.A., Z.C., and Y.C; Z.C. performed in vivo transplantation with old donor mice; E.M.A. and B.H. performed in vivo transplantation with young donor mice; M.K.R. and A.L.M. performed computational data analyses of bulk and scRNA-seq; K.S. gave support in statistical analysis; S.R.C. generated the knockout-construct for genome targeting in embryonic stem cells, and B.O.B. designed and supported the study; and K.L.R. designed and supervised the study and wrote the manuscript.

Conflict-of-interest disclosure: The authors declare no competing financial interests.

The current affiliation for S.R.C. is Department of Health Research-Multidisciplinary Research Unit (DHR-MRU), Dr. A.L.M. Postgraduate (PG) Institute of Basic Medical Sciences, University of Madras, Chennai, India.

ORCID profiles: M.K.R., 0000-0003-3071-7419; K.S., 0000-0001-6391-1766; B.O.B., 0000-0002-2706-7710; A.L.M., 0000-0003-0689-7907; K.L.R., 0000-0002-4839-2862.

Correspondence: K. Lenhard Rudolph, Leibniz Institute on Aging, Fritz Lipmann Institute (FLI), Beutenbergstr. 11, 07745 Jena, Germany; e-mail: lenhard.rudolph@leibniz-fli.de.

Footnotes

REFERENCES

1. Shyh-Chang N, Daley GQ, Cantley LC. Stem cell metabolism in tissue development and aging. *Development*. 2013;140(12):2535-2547.

2. Ren R, Ocampo A, Liu GH, Izpisua Belmonte JC. Regulation of stem cell aging by metabolism and epigenetics. *Cell Metab*. 2017;26(3):460-474.

3. Brunet A, Rando TA. Interaction between epigenetic and metabolism in aging stem cells. *Curr Opin Cell Biol*. 2017;45:1-7.

4. Luo H, Mu WC, Karki R, et al. Mitochondrial stress-initiated aberrant activation of the NLRP3 inflammasome regulates the functional deterioration of hematopoietic stem cell aging. *Cell Rep*. 2019;26(4):945-954.e4.

5. Chen C, Liu Y, Liu Y, Zheng P. mTOR regulation and therapeutic rejuvenation of aging hematopoietic stem cells. *Sci Signal*. 2009;2(98):ra75.

6. Signer RA, Magee JA, Salic A, Morrison SJ. Haematopoietic stem cells require a highly regulated protein synthesis rate. *Nature*. 2014;509(7498):49-54.

7. Shyh-Chang N, Daley GQ. Lin28: primal regulator of growth and metabolism in stem cells. *Cell Stem Cell*. 2013;12(4):395-406.

8. Zhang J, Ratanasirintrawoot S, Chandrasekaran S, et al. LIN28 regulates stem cell metabolism and conversion to primed pluripotency. *Cell Stem Cell*. 2016;19(1):66-80.

9. Zhu H, Shyh-Chang N, Segrè AV, et al; MAGIC Investigators. The Lin28/let-7 axis regulates glucose metabolism. *Cell*. 2011;147(1):81-94.

10. Bell JL, Wächter K, Mühleck B, et al. Insulin-like growth factor 2 mRNA-binding proteins (IGF2BPs): post-transcriptional drivers of cancer progression? *Cell Mol Life Sci.* 2013; 70(15):2657-2675.

11. Nielsen J, Christiansen J, Lykke-Andersen J, Johnsen AH, Wewer UM, Nielsen FC. A family of insulin-like growth factor II mRNA-binding proteins represses translation in late development. *Mol Cell Biol.* 1999;19(2): 1262-1270.

12. Li Z, Gilbert JA, Zhang Y, et al. An HMGA2-IGF2BP2 axis regulates myoblast proliferation and myogenesis [published correction appears in *Dev Cell.* 2013;24(1):112]. *Dev Cell.* 2012;23(6):1176-1188.

13. Schaeffer V, Hansen KM, Morris DR, LeBoeuf RC, Abrass CK. RNA-binding protein IGF2BP2/IMP2 is required for laminin-β2 mRNA translation and is modulated by glucose concentration. *Am J Physiol Renal Physiol.* 2012;303(1): F75-F82.

14. Dai N, Zhao L, Wrighting D, et al. IGF2BP2/IMP2-deficient mice resist obesity through enhanced translation of Ucp1 mRNA and other mRNAs encoding mitochondrial proteins. *Cell Metab.* 2015;21(4):609-621.

15. Mineo M, Ricklefs F, Rooj AK, et al. The long non-coding RNA HIF1A-AS2 facilitates the maintenance of mesenchymal glioblastoma stem-like cells in hypoxic niches. *Cell Rep.* 2016;15(11):2500-2509.

16. Gong C, Li Z, Ramanujan K, et al. A long non-coding RNA, LncMyoD, regulates skeletal muscle differentiation by blocking IMP2-mediated mRNA translation. *Dev Cell.* 2015; 34(2):181-191.

17. Yuan J, Nguyen CK, Liu X, Kanellopoulou C, Muljo SA. Lin28b reprograms adult bone marrow hematopoietic progenitors to mediate fetal-like lymphopoiesis. *Science.* 2012;335(6073):1195-1200.

18. Copley MR, Babovic S, Benz C, et al. The Lin28b-let-7-Hmga2 axis determines the higher self-renewal potential of fetal haematopoietic stem cells. *Nat Cell Biol.* 2013; 15(8):916-925.

19. Pietras EM, Passegué E. Linking HSCs to their youth [published correction appears in *Nat Cell Biol.* 2013;15(9):1131]. *Nat Cell Biol.* 2013;15(8):885-887.

20. Chaudhuri AA, So AY, Mehta A, et al. Oncomir miR-125b regulates hematopoiesis by targeting the gene Lin28A. *Proc Natl Acad Sci USA.* 2012;109(11):4233-4238.

21. Khurana S, Buckley S, Schouteden S, et al. A novel role of BMP4 in adult hematopoietic stem and progenitor cell homing via Smad independent regulation of integrin-α4 expression. *Blood.* 2013;121(5):781-790.

22. Morita Y, Ema H, Nakauchi H. Heterogeneity and hierarchy within the most primitive hematopoietic stem cell compartment. *J Exp Med.* 2010;207(6):1173-1182.

23. Flohr Svendsen A, Yang D, Kim K, et al. A comprehensive transcriptome signature of murine hematopoietic stem cell aging. *Blood.* 2021 138(6):439-451.

24. Yu JSL, Cui W. Proliferation, survival and metabolism: the role of PI3K/AKT/mTOR signalling in pluripotency and cell fate determination. *Development.* 2016;143(17): 3050-3060.

25. Ghosh J, Kapur R. Regulation of hematopoietic stem cell self-renewal and leukemia maintenance by the PI3K-mTORC1 pathway. *Curr Stem Cell Rep.* 2016;2(4): 368-378.

26. Mu Q, Wang L, Yu F, et al. Imp2 regulates GBM progression by activating IGF2/PI3K/Akt pathway. *Cancer Biol Ther.* 2015;16(4): 623-633.

27. Cao J, Mu Q, Huang H. The roles of insulin-like growth factor 2 mRNA-binding protein 2 in cancer and cancer stem cells. *Stem Cells Int.* 2018;2018:4217259.

28. Calvanese V, Nguyen AT, Bolan TJ, et al. MLLT3 governs human haematopoietic stem-cell self-renewal and engraftment. *Nature.* 2019;576(7786):281-286.

29. Matsumoto A, Takeishi S, Kanie T, et al. p57 is required for quiescence and maintenance of adult hematopoietic stem cells. *Cell Stem Cell.* 2011;9(3):262-271.

30. Balazs AB, Fabian AJ, Esmon CT, Mulligan RC. Endothelial protein C receptor (CD201) explicitly identifies hematopoietic stem cells in murine bone marrow. *Blood.* 2006;107(6): 2317-2321.

31. Liu L, Zhao M, Jin X, et al. Adaptive endoplasmic reticulum stress signalling via IRE1α-XBP1 preserves self-renewal of haematopoietic and pre-leukaemic stem cells. *Nat Cell Biol.* 2019;21(3):328-337.

32. Warsi S, Dahl M, Rorby E, et al. Schlafen2 Is a critical regulator of adult hematopoietic stem cells [abstract]. *Exp Hematol.* 2016; 44(9). Abstract S49.

33. Venkatraman A, He XC, Thorvaldsen JL, et al. Maternal imprinting at the H19-Igf2 locus maintains adult haematopoietic stem cell quiescence. *Nature.* 2013;500(7462): 345-349.

34. Sommerkamp P, Renders S, Ladel L, et al. The long non-coding RNA Meg3 is dispensable for hematopoietic stem cells. *Sci Rep.* 2019;9(1):2110.

35. Kimball SR. Eukaryotic initiation factor eIF2. *Int J Biochem Cell Biol.* 1999;31(1):25-29.

36. Signer RA, Qi L, Zhao Z, et al. The rate of protein synthesis in hematopoietic stem cells is limited partly by 4E-BPs. *Genes Dev.* 2016;30(15):1698-1703.

37. Maryanovich M, Zaltsman Y, Ruggiero A, et al. An MTCH2 pathway repressing mitochondria metabolism regulates haematopoietic stem cell fate. *Nat Commun.* 2015;6(1):7901.

38. Chen C, Liu Y, Liu R, et al. TSC-mTOR maintains quiescence and function of hematopoietic stem cells by repressing mitochondrial biogenesis and reactive oxygen species. *J Exp Med.* 2008;205(10): 2397-2408.

39. Morrison SJ, Wandycz AM, Akashi K, Globerson A, Weissman IL. The aging of hematopoietic stem cells. *Nat Med.* 1996; 2(9):1011-1016.

40. De Haan G, Van Zant G. Genetic analysis of hemopoietic cell cycling in mice suggests its involvement in organismal life span. *FASEB J.* 1999;13(6):707-713.

41. Sudo K, Ema H, Morita Y, Nakauchi H. Age-associated characteristics of murine hematopoietic stem cells. *J Exp Med.* 2000; 192(9):1273-1280.

42. Pang WW, Price EA, Sahoo D, et al. Human bone marrow hematopoietic stem cells are increased in frequency and myeloid-biased with age. *Proc Natl Acad Sci USA.* 2011; 108(50):20012-20017.

43. Gekas C, Graf T. CD41 expression marks myeloid-biased adult hematopoietic stem cells and increases with age. *Blood.* 2013; 121(22):4463-4472.

44. Haas S, Hansson J, Klimmeck D, et al. Inflammation-induced emergency megakaryopoiesis driven by hematopoietic stem cell-like megakaryocyte progenitors. *Cell Stem Cell.* 2015;17(4):422-434.

45. Yamamoto R, Wilkinson AC, Ooehara J, et al. Large-scale clonal analysis resolves aging of the mouse hematopoietic stem cell compartment. *Cell Stem Cell.* 2018; 22(4):600-607.e4.

46. Beerman I, Bhattacharya D, Zandi S, et al. Functionally distinct hematopoietic stem cells modulate hematopoietic lineage potential during aging by a mechanism of clonal expansion. *Proc Natl Acad Sci USA.* 2010;107(12):5465-5470.

47. Cabezas-Wallscheid N, Klimmeck D, Hansson J, et al. Identification of regulatory networks in HSCs and their immediate progeny via integrated proteome, transcriptome, and DNA methylome analysis. *Cell Stem Cell.* 2014;15(4):507-522.

48. Pietras EM, Reynaud D, Kang YA, et al. Functionally distinct subsets of lineage-biased multipotent progenitors control blood production in normal and regenerative conditions. *Cell Stem Cell.* 2015;17(1): 35-46.

49. Yin R, Chang J, Li Y, et al. Differential m^{6}A RNA landscapes across hematopoiesis reveal a role for IGF2BP2 in preserving hematopoietic stem cell function. *Cell Stem Cell.* 2022;29(1):149-159.e7.

50. Perez-Riverol Y, Csordas A, Bai J, et al. The PRIDE database and related tools and resources in 2019: improving support for quantification data. *Nucleic Acids Res.* 2019; 47(D1):D442-D450.